RF DESIGN AND TUNING OF LINAC4 RFQ

A.C. France, M. Desmons, O. Piquet, CEA Saclay, France
C. Rossi, CERN, Geneva, Switzerland

Abstract

Linac4 is scheduled to deliver 160 MeV H$^-$ beam to LHC injection chain by year 2015. The first stage of Linac4 is a 352 MHz, 3-meter long Radio Frequency Quadrupole (RFQ) accelerator [1]. It will accelerate the 70 mA, 45 keV H$^-$ beam from the RF source up to 3 MeV energy. Fabrication of RFQ, which started in 2009, is completed [2] and tuning operations are in progress. RF controls performed at each fabrication step have shown that RFQ electrical parameters are well within bounds specified after envelope of fabrication tolerances. Tuning operations have started with adjustment of so-called quadrupole rods inserted in end plates, in order to achieve adequate voltage boundary conditions at both RFQ ends. A preliminary slug tuning test demonstrates voltage percent accuracy after a few slug tuning iterations.

RF DESIGN

Linac4 RFQ is a 3-meter long, single segment RFQ. Cross-section is kept constant over full RFQ length, in order to simplify mechanical fabrication (refer to [3] for detailed RF design). Specified voltage is constant over full RFQ length, and boundary conditions are tuned with quadrupole rods (QR) inserted in end plates, close to vane tips. Electrical parameters of RFQ however vary slightly vs. abscissa, as a consequence of vane modulations. Resulting voltage error is 10% at most, and will be easily suppressed with the 36 tuners (8 slugs and 1 RF port per quadrant). Tuners are also designed to compensate for construction errors. Envelope of fabrication tolerances may yield inter-vane capacitance errors of 2.3% (quadrupole-like errors) and/or 3.5% (dipole-like errors). The resulting tuner position range is about 34 mm, and is centered mostly "inside cavity", where tuner are efficient. To this purpose resonance frequency is set to 345.3 MHz when tuners are in flush position.

THEORETICAL BACKGROUND

A general statement is that RFQ tuning requires some bridge to be made between the 3D field maps of the desired object, and measurable quantities which are field profiles along bead-pull lines and spectra. This bridge is the 4-wire transmission line model (TLM) described in [4]. Field maps in the axial region of a 4-vane RFQ may be approximated by transverse electric-magnetic (TEM) field maps, since there the axial component of magnetic field is close to zero. These TEM field maps are assumed to be supported by a 4-wire system, whose voltage 3-vector U verifies

$$\frac{\partial}{\partial z}\left(C_Q \frac{\partial U}{\partial z}\right) + \frac{1}{c^2} L_Q U = \frac{\omega^2}{c^2} C_Q U , \qquad (1)$$

where z is abscissa, C_Q, L_Q are the capacitance (F/m) and inductance (H.m) matrixes, ω is the radian frequency, c is the speed of light. Quadrupole (U_Q) and dipole (U_S,U_T) components of U are related to inter-electrode voltages by $U_Q =(u_1–u_2+u_3–u_4)/4$, $U_S = (u_1–u_3)/2$, $U_T = (u_2–u_4)/2$. Note that (1) is diagonal for a perfectly symmetric RFQ. Boundary conditions at RFQ ends in z = a,b are

$$\partial U(a)/\partial z = -s_a U(a) \; , \quad \partial U(b)/\partial z = +s_b U(b) , \qquad (2)$$

where s_a, s_b are 3×3 matrixes. The vector Sturm-Liouville (SL) operator defined after (1) and (2) is self-adjoint if and only if $(C_Q)^{-1}s_{a,b}$ are Hermitian, which is always the case since $s_{a,b} = –j(\omega/c^2)C_Q^{-1}y_{a,b}$, where $y_{a,b}$ are end-circuit admittance matrixes, and are imaginary symmetric for lossless reciprocal circuits. All TLM electrical parameters are deduced from exact 3D simulations [3], in such a way TLM is able to accurately mimic RFQ eigen-modes and eigen-functions. On the other hand, magnetic field measured along bead-pull lines are easily transformed into inter-vane voltage (eventually using simulated field maps), eigen-values $(\omega/c)^2$ are directly given by spectrum analysis, and our "bridge" is established. First-order perturbation analysis of the SL eigen-problem leads to orthogonal bases for C_Q and L_Q perturbations, which are duals of voltage eigen-basis. This important property will be applied for RF controls and for slug tuning.

RF CONTROLS

RF controls are performed at each fabrication step of each 1-meter long section: copper pieces assembly, first braze of electrodes, second braze of stainless flanges and vacuum ports. The most desirable goal would be to obtain a diagnosis of electrical properties vs. abscissa along the RFQ. This is a typical inverse problem: given voltage vector function U(z), find originating $C_Q(z)$ matrix pencil. The hard point is that U may be deduced from measured magnetic field only in small intervals, far enough from local field perturbations induced by tuners and vacuum ports. Applying sampling theory to our SL problem, a linear filter bank may be built which uses valid field samples to deliver a few spectral amplitudes estimates (6 first in present case). First-order perturbation analysis is then used to reconstruct originating perturbations. This method is of course unable to reveal strongly localized defaults; however the same procedure will be used for tuning, and these estimated perturbations are exactly the ones that will have to be cancelled by tuners. Results are displayed in Fig. 1, where successive fabrication steps are identified with color code. Typical precision of the method is ±0.003, after processing typically 5 or 6 bead-pulls. A digital "roofing" filter is also used to reduce high-frequency noise. Black traces apply to the full-length

assembled RFQ, and nicely follow individual 1-meter long sections estimates. All capacitance errors never exceed 1%, well within specifications. Note that vacuum ports positions are adjusted prior to second braze, as explained in [5]. A similar procedure is used to estimate electrical neutral position of RF dummy ports (which was not perfect after assembly, but was corrected later on as can be seen in Fig. 1, about z = 1.50 m).
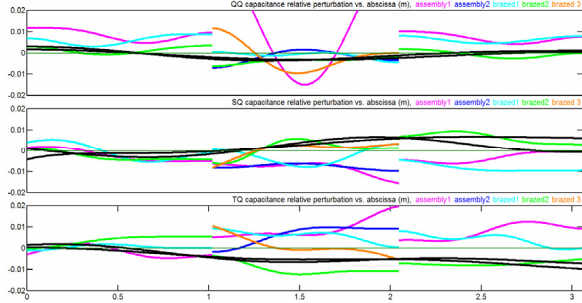
Figure 1: Reconstruction of inter-vane capacitance errors vs. abscissa along RFQ axis and fabrication step (color).

END-CIRCUITS TUNING

Coefficients of $s_{a,b}$ matrixes are estimated using the excitation set method. Several linearly independent $\{U, \partial U/\partial z\}|_{z=a,b}$ pairs are obtained upon prepositioning tuners # 04 and 06 (on either side of central RF port). End voltages and voltage slopes are derived from bead-pull measurements. Straightforward linear algebra shows that a minimum of three pairs is sufficient to recover all coefficients. Accuracy is improved upon using five pairs (as shown in Table 1) and least-square fit. The symmetry of the dipole sub-matrix $[s_{SS} \; s_{ST} \; ; \; s_{ST} \; s_{TT}]$ is also taken into account.

Table 1: Positions (in mm) of Tuners 04 and 06

excitation	quad 1	quad 2	quad 3	quad 4
f	0.0	0.0	0.0	0.0
s	+5.0	0.0	–0.5	0.0
y	+5.0	+5.0	–0.5	–0.5
t	0.0	+5.0	0.0	–0.5
x	–0.5	+5.0	–0.5	+5.0

Results of a typical measurement are displayed in Fig. 2. Left plot is a visual representation in $\{U_Q, \partial U_Q/\partial z\}$ plane; in this un-tuned case, $s_{QQ} = +0.106$ V/m/V (tuned value is 0, since required voltage profile is constant). Right plot is a superposition of $\{U_S, U_T\}$ and $\{\partial U_S/\partial z, \partial U_T/\partial z\}$ planes. Voltage excitations (blue circles) are easily identified (f-excitation is not exactly quadrupolar since RFQ is not tuned). Measured voltage slopes are shown with green +. Voltage slopes derived from measured voltages and estimated s-matrix are shown with purple ×. They closely track measured samples, indicating that s-matrix parameters have been properly estimated. Note also that principal axes in dipole subspace are of little importance for tuning, to the contrary of eigen-values that will determine dipole eigen-frequencies. Status of end-circuits tuning is displayed in Fig. 3. Most

recent Comsol 3D simulations are shown in blue; measured values in green and red. Left plots apply to RFQ input; right ones to RFQ output. Top plots display s_{QQ} values vs. QR length; vertical bars represent ±1 standard deviation intervals (if available). Bottom plots display mean eigen-value λ_D of dipole sub-matrix vs. QR length; vertical bars represent eigen-value separation intervals. s_{QQ} tuning curves at RFQ input (in green on Fig. 3, top-left) and output (in red on Fig. 3, top-right) are measured using aluminum end-plates with adjustable rods, and closely match simulations; same conclusion applies to realized input copper plate (in red on Fig. 3, top-left). Measured λ_D closely match simulation for shorter rods, but do not follow the same slope. This apparent discrepancy likely results from ignored dispersive effects, simulated λ_D's applying to dipole mode fundamental frequency and measured values to quadrupole mode fundamental frequency. Note that $s_{a,b}$ are assumed to be independent of frequency in TLM (eigen-value dependent boundary conditions may be treated to the expense of heavy bead-pull measurements as in [6]). A definitive conclusion could be reached upon considering spectra of RFQ once tuned (eigen-frequencies being usually shifted by electrical parameters errors not compensated by tuners).
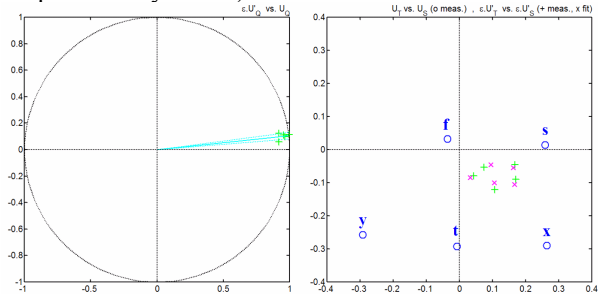
Figure 2: Example of end-circuit tuning (RFQ output).
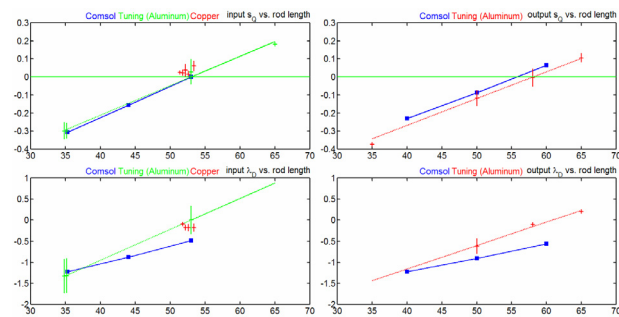
Figure 3: Summary of end-circuits tuning.

SLUG TUNING TEST

A slug tuning test has been performed with input copper plate and output aluminum plate. The closed-loop control-command tuning algorithm is sketched out in Fig. 4. A linear filter-bank derives voltage spectral components (12 in each Q, S, T subset in the present case) from valid measured samples (the controlled quantities). First-order perturbation analysis of SL operator is used to build the dual basis of tuner functions (with dim. 9 in

each subset). Measured spectral coefficients are compared to desired ones (i.e. spectral coefficients of specified voltage function in quadrupole subset, all zeroes in dipole subsets). Inverse RFQ transfer function is then applied to elaborate command parameters in each spectral channel. Transmittance of linear filter bank and normalized spectra of tuner basis functions are displayed in Fig. 5; it is seen that 8 first components are free from aliasing hence tunable.
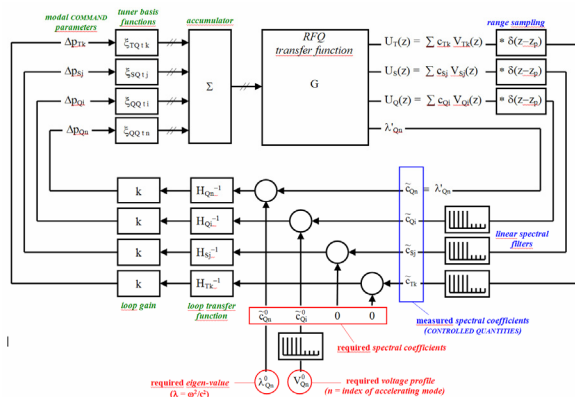
Figure 4: Tuning algorithm.
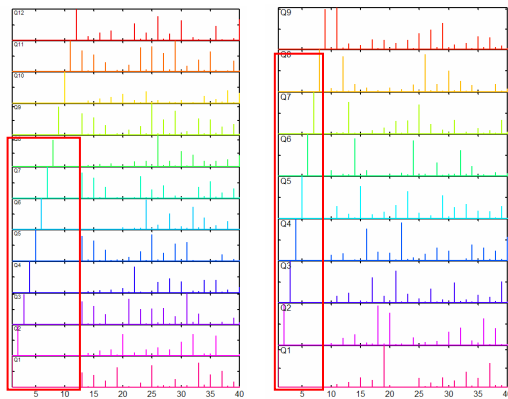
Figure 5: Transmittance of linear filter bank (left), and normalized spectra of tuner basis functions (right).

Table 2: Summary of Tuning Test Iterations

	step 0		step 5	
frequency (MHz)	345.741		351.926	
Q-component error (%)	−22.77	+18.72	−1.24	+0.77
S-component error (%)	−5.29	+8.13	−0.05	+1.29
T-component error (%)	+1.73	+7.97	−0.98	+3.06
tuner positions (mm)	0.00		+5.07	+13.42

After 5 tuning iterations, voltage errors are reduced from 23% down to a few percents (Table 2 and Fig. 6). More iterations are expected to yield better voltage accuracy and frequency match. Tuner positions vary between +5 and +13.4 mm (inside cavity), well within the [−4,+30.5] mm specification, and in agreement with small measured capacitance errors. Frequencies of dipole modes closer to accelerating Q_0 mode are given in Table 3 (acquisition step, hence accuracy, is 62.5 kHz). TLM values are derived using measured s-matrix coefficients,

and assuming tuners in neutral position; quadratic frequency shifts (QFS) should theoritically be left unchanged by frequency tuning. After tuning, QFS are quite close to those derived from TLM, thus indirectly confirming our s-matrix estimates.
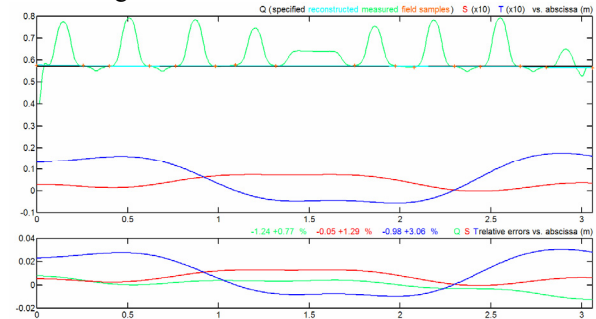
Figure 6: Voltage profile after last tuning step.

Table 3: Spectrum Analysis of Tuning Iterations

	step 0			step 5			TLM		
	f	QFS	Δf	f	QFS	Δf	f	QFS	Δf
D_0	333.38	−91.7	−12.4	339.13	−94.1	−12.8	332.56	−94.0	−13.0
D_1	339.19	−67.0	−6.6	345.00	−69.5	−6.9	338.11	−71.5	−7.5
Q_0	345.75	0.0	0.0	351.94	0.0	0.0	345.59	0.0	0.0
D_2	349.13	+48.4	+3.4	354.25	+40.4	+2.3	348.14	+42.0	+2.5
D_3	364.94	+116.8	+19.2	369.88	+113.8	+17.9	365.34	+118.5	+19.7

CONCLUSION

End-circuits tuning is now almost completed; fabrication of copper output plate is underway. End-circuits modeling is found to be satisfactory in quadrupole subspace, but deserves finer analysis in dipole subspace. A tuning test clearly demonstrates that required tuner position range is largely within specifications, in agreement with estimated inter-vane capacitance errors. Next tuning steps include: assembly of output copper plate and tuning check, tuning with dummy slugs and dummy RF ports, assembly and matching of iris coupler, fabrication and assembly of copper iris coupler, final tuning and fabrication of copper slugs.

REFERENCES

[1] C. Rossi et al., "The Radiofrequency Quadrupole Accelerator for the Linac4", LINAC'08, Victoria BC, Canada.

[2] C. Rossi et al., "Assembly and RF Tuning of the Linac4 RFQ at CERN", LINAC'12, Tel Aviv, Israel.

[3] O. Piquet et al., "The RF Design of the Linac4 RFQ" IPAC'10, Kyoto, Japan.

[4] A.C. France et al., "Un-segmented vs. Segmented 4-vane RFQ: Theory and Cold Model Experiments", IPAC'10, Kyoto, May 2010, MOPD026.

[5] C. Rossi et al., "Progress in the Fabrication of the RFQ Accelerator for the CERN Linac4," LINAC'10, Tsukuba, Japan.

[6] O. Piquet et al., "Tuning Procedure of the 6-Meter IPHI RFQ", EPAC'06, Edimburgh, U.K., MOPCH107.